10-2000

Time series analysis of V815 Herculis photometry between 1984 and 1998

Lauri Jetsu
University of Helsinki

Thomas Hackman
University of Helsinki

Douglas S. Hall
Vanderbilt University

Gregory W. Henry
Tennessee State University

Mariitta Kokko
University of Helsinki

See next page for additional authors

Astron. Astrophys. 362, 223–235 (2000)

ASTRONOMY AND ASTROPHYSICS

Time series analysis of V815 Herculis photometry between 1984 and 1998⋆

L. Jetsu[1], **T. Hackman**[1], **D.S. Hall**[2], **G.W. Henry**[3], **M. Kokko**[1], **and J. You**[4]

[1] Observatory, P.O. Box 14, 00014 University of Helsinki, Finland
[2] Dyer Observatory, Vanderbilt University, Nashville, TN 37235, USA
[3] Center of Excellence in Information Systems, Tennessee State University, 330 10th Ave. North, Nashville, TN 37203-3401, USA
[4] Astronomy Division, P.O. Box 3000, 90014 University of Oulu, Finland

Received 17 December 1999 / Accepted 14 August 2000

Abstract. As a case study of the solar-stellar connection, we have analysed a prolonged time series of BV photometry of the chromospherically active binary V815 Her. The surface differential rotation in the rapidly rotating G5V primary caused changes of 4.6% in the seasonal photometric rotation periods. This would imply a differential rotation coefficient of $k = 0.184$, if the rotation of the starspots follows the solar law of differential rotation and the activity is confined within the same latitudinal range as in the Sun, having $k = 0.189$ and the spectral-type of G2V. Our analysis of the primary and secondary minima of the seasonal light curves indicated that the regions of stronger activity have concentrated on one active longitude, which has maintained a constant rotation period of $1.^{\rm d}79244$ for about 14 years. No regular activity cycle was detected in the mean brightness changes of V815 Her.

Key words: stars: individual: V815 Her – stars: variables: general – stars: activity – techniques: photometric

1. Introduction

Heard (1956) discovered the radial velocity variations of the single-lined G5 V/M1-2 V binary V815 Her (HD 166181). Nadal et al. (1974) noticed the strong CaII H&K emission, determined the orbital period $P_{\rm orb} = 1.^{\rm d}8098368$ and the absolute magnitude $M_{\rm V} = 5.2$ of the G5V primary. Their orbital elements gave $i > 40°$, while the absence of eclipses implied $i < 78°$. The conclusion by Nadal et al. (1974), that the G5V primary is the more active component, was confirmed later (Fernandez-Figueroa 1986; Fekel et al. 1986; Dempsey et al. 1996). Eggen (1978) detected the photometric variability of V815 Her, which is most probably caused by starspots on the surface of the primary. The subsequent photometry by Mekkadan et al. (1980) revealed nearly synchronized orbital motion and rotation. Strassmeier et al. (1989) obtained $P_{\rm phot} = 1.^{\rm d}8195$ and $1.^{\rm d}8365$ from their 1985 and 1986 photometry.

The rapid rotation, $v \sin i = 27 {\rm km\ s^{-1}}$, was measured by Fekel et al. (1986), who also noticed the strong lithium line, indicating that the primary is a young star. Liu et al. (1993) and Barrado y Navascues et al. (1997) have later observed this LiI 6707.8Å line in V815 Her. Dempsey et al. (1996) made new radial velocity measurements and refined the orbital period to $P_{\rm orb} = 1.^{\rm d}8098355 \pm 0.^{\rm d}0000021$. They suggested that an undetected third body having an orbital period of many years may be present in the V815 Her system, because their revised orbital elements agreed with those in Nadal et al. (1974), except for a large offset in the mean of the radial velocities. Combining $P_{\rm phot} = 1.^{\rm d}8$ with the recently revised $v \sin i = 31.2 {\rm km\ s^{-1}}$ gives a minimum radius of $R \geq 1.1 R_{\odot}$ for the primary (Fekel 1997). Assuming no interstellar extinction, the Hipparcos satellite 32.6 pc distance estimate (Perryman et al. 1997) and the $V = 7.7$ mean apparent magnitude indicate an absolute magnitude $M_{\rm V} = 5.1$, which agrees with the earlier estimates of $M_{\rm V} = 5.2$ (Nadal et al. 1974; Eggen 1978).

Several signatures of magnetic activity have been detected in V815 Her: choromospheric, transition region and coronal emission from the radio to the X-ray wavelengths. The ground-based observations consist of the CaII H&K, Hα and other chromospheric emission line measurements at the optical wavelengths (e.g. Bopp 1984; Fernandez-Figueroa et al. 1986; Fekel et al. 1986; Eker et al. 1995; Dempsey et al. 1996; Montes et al. 1997) and of coronal emission measurements at the radio wavelengths (e.g. Drake et al. 1986, 1992; Gunn et al. 1994). The satellite observations include measurements in the ultraviolet (IUE: Fekel et al. 1986; Simon & Fekel 1987; Dempsey et al. 1996), the extreme ultraviolet (EUVE: Malina et al. 1994; Mitrou et al. 1997) and the X-ray (ROSAT: Pounds et al. 1993; Dempsey et al. 1993a, 1993b). However, the detection of V815 Her in the 12 μm-band of the IRAS satellite is not necessarily connected to magnetic activity (Mitrou et al. 1996). Dempsey et al. (1996) observed no rotational modulation in the optical chromospheric emission lines, but noted that the UV emission varied roughly in antiphase with the contemporary V light curve. Two flares having a duration of 10.4 and 21.1 hours were recently iden-

Send offprint requests to: L. Jetsu (Lauri.Jetsu@astro.helsinki.fi)

⋆ Table 1 is available only in electronic form at CDS via anonymous ftp to edarc.u-strasbg.fr (130.79.1285) or via http: //cdsweb.u-strasbg.fr/Abstract.html. These data are also available at http: //schwab.tsuniv.edu/t3/v815her/v815her.html

tified in the EUVE light curves of V815 Her (Osten & Brown 1999).

We analysed a time series of photometry of V815 Her between 1984 and 1998. The published and new data described in Sect. 2 have been compiled into our Table 1, which is published *only* in electronic form.[1] This table gives the subsets (1st column: SET), the heliocentric Julian dates (2nd column: HJD) and the differential BV magnitudes V815 Her minus the comparison star HD 166093 (3rd and 4th columns). The topics of Sect. 3 are: the light curve modelling with a variable photometric rotation period, the short- and long-term luminosity changes, the surface differential rotation and the active longitudes. Conclusions are presented in Sect. 4.

2. Observations

We studied the BV photometry of V815 Her obtained with two Automatic Photoelectric Telescopes (APT) between 1984 and 1998. Since the light curves of V815 Her did not undergo significant changes during ten rotations (see Sect. 3.2), these data have been divided into 98 separate subsets with an average length of about 20 days (Table 2: SET). This ensured an adequate light curve phase coverage with the photometric rotation period of $P_{\rm phot} \approx 1.^{\rm d}8$.

The first subsets SET=1–22 contain the *earlier* published BV differential photometry of V815 Her, which was made with the Phoenix 0.25m APT (Strassmeier et al. 1989). The comparison star was HD 166093. These APT observations began at Phoenix, Arizona (SET=1–15). In summer 1986 this telescope was relocated to Mount Hopkins, Arizona (SET=16–22).

The other subsets SET=23–98 contain the *new* BV differential photometry made with the Vanderbilt-Tennessee State 0.4m APT. In summer 1996 this APT was relocated from Mount Hopkins (SET=23–85) to Washington Camp, Arizona (SET=86–98). The comparison and check stars were HD 166093 and HD 166014, respectively. The observations were corrected for differential extinction and transformed to the standard Johnson system. Each observation is a mean of three measurements. All observations with a standard deviation greater than $0.^{\rm m}02$ were automatically rejected during the first part of these new data. This criterion was reduced to $0.^{\rm m}01$ in spring 1992, because the data quality improved after installing a new precision photometer. More detailed information about the automatic telescope photometry can be found in Henry (1995a, 1995b).

We used the detection procedure from Jetsu et al. (1993) to search for flares in V815 Her. Henry & Newsom (1996) applied a similar technique to the earlier APT photometry of 69 chromospherically active stars from Strassmeier et al. (1989). They detected flares only in three stars, UX Ari, II Peg and AR Psc, but none in V815 Her. We found no evidence for photometric flares in any of the data subsets in Table 1.

The B and V magnitude differences between HD 166014 and HD 166093 give an estimate of the precision of these data. Before spring 1992 the standard deviations *within* each year were $0.^{\rm m}015$ in V and $0.^{\rm m}017$ in B. The respective estimates improved to $0.^{\rm m}006$ and $0.^{\rm m}007$ with the new precision photometer. The external accuracy mentioned in Henry et al.

[1] Note that Table 2 is the first table appearing in this paper, because Table 1 is published *only* in electronic form.

Table 2. The subsets (SET) of the BV photometry of V815 Her: the observing time interval, and the number of observing nights in V and B ($N_{\rm V}$ and $N_{\rm B}$)

SET	Interval	$N_{\rm V}$	$N_{\rm B}$	SET	Interval	$N_{\rm V}$	$N_{\rm B}$
1	27.9.-20.10.1984	8	9	50	9.-29.4.1992	12	12
2	23.10.-10.11.1984	12	12	51	3.-25.5.1992	9	11
3	11.2.-5.3.1985	14	14	52	19.6.-6.7.1992	11	11
4	13.3.-3.4.1985	12	12	53	9.9.-2.10.1992	15	14
5	5.-25.4.1985	14	14	54	3.-26.10.1992	12	13
6	29.4.-22.5.1985	10	10	55	2.-18.11.1992	12	12
7	23.5.-15.6.1985	19	19	56	21.1.-7.2.1993	7	7
8	16.6.-13.7.1985	15	15	57	5.-25.3.1993	11	11
9	23.7.-10.8.1985	11	11	58	31.3.-20.4.1993	12	12
10	12.-30.8.1985	13	13	59	24.4.-13.5.1993	16	16
11	4.-25.9.1985	17	17	60	17.5.-5.6.1993	18	18
12	30.9.-21.10.1985	11	11	61	7.-28.6.1993	21	21
13	22.10.-14.11.1985	10	10	62	4.9.-3.10.1993	16	15
14	30.4.-29.5.1986	13	13	63	24.10.-10.11.1993	9	8
15	5.-27.6.1986	18	18	64	21.1.-16.2.1994	10	10
16	29.9.1986	1	1	65	23.2.-23.3.1994	13	13
17	3.-24.3.1987	9	9	66	28.3.-16.4.1994	11	11
18	2.-25.4.1987	15	15	67	22.4.-17.5.1994	19	19
19	3.-28.5.1987	9	9	68	19.5.-15.6.1994	19	18
20	15.6.-7.7.1987	14	14	69	23.6.-12.7.1994	10	10
21	1.-27.10.1987	12	12	70	13.-31.10.1994	10	12
22	8.-12.11.1987	4	4	71	5.-29.11.1994	9	9
23	16.11.1987	1	1	72	29.1.-25.2.1995	11	11
24	25.4.-8.5.1988	13	11	73	9.3.-3.4.1995	16	17
25	14.-29.5.1988	11	13	74	8.-26.4.1995	13	14
26	31.5.-17.6.1988	15	15	75	3.-24.5.1995	11	12
27	13.9.-16.10.1988	20	19	76	27.5.-18.6.1995	14	17
28	23.10.-18.11.1988	16	14	77	19.6.-11.7.1995	20	19
29	10.-27.2.1989	9	5	78	22.9.-15.10.1995	20	21
30	8.-29.3.1989	13	13	79	16.10.-5.11.1995	16	16
31	30.3.-19.4.1989	17	17	80	8.-29.11.1995	12	12
32	20.4.-8.5.1989	13	13	81	29.1.-2.3.1996	10	10
33	12.-31.5.1989	15	16	82	7.3.-4.4.1996	12	12
34	3.-25.6.1989	14	16	83	8.4.-4.5.1996	23	23
35	10.9.-2.10.1989	13	12	84	5.-31.5.1996	19	19
36	8.-25.10.1989	7	10	85	1.-27.6.1996	15	15
37	28.10.-15.11.1989	9	10	86	5.-26.11.1996	12	13
38	4.-24.2.1990	8	8	87	1.-24.2.1997	13	13
39	28.2.-25.3.1990	9	9	88	3.-28.3.1997	19	20
40	6.4.-1.5.1990	10	11	89	1.-23.4.1997	14	16
41	4.-30.5.1990	14	17	90	24.4.-14.5.1997	12	13
42	31.5.-25.6.1990	17	16	91	22.5.-16.6.1997	14	15
43	13.10.-15.11.1990	14	12	92	19.6.-13.7.1997	16	16
44	14.2.-9.3.1991	5	6	93	20.9.-19.10.1997	18	19
45	7.-27.4.1991	11	12	94	24.10.-30.11.1997	16	17
46	29.4.-18.5.1991	13	12	95	15.1.-12.2.1998	11	13
47	21.5.-8.6.1991	13	17	96	23.2.-11.3.1998	11	11
48	11.6.-2.7.1991	14	15	97	20.3.-21.4.1998	25	25
49	15.-26.3.1992	5	6	98	22.4.-23.5.1998	18	18

(1995a) equals the standard deviation of $0.^{\rm m}003$ *between* the yearly means both in V and B. Therefore the yearly means after spring 1992 provide the most reliable estimates of the magnitude differences between HD 166014 and HD 166093: $\Delta V = -3.358 \pm 0.003$ and $\Delta B = -4.706 \pm 0.003$. The comparison and/or check star may be weakly variable, because the standard deviations within each year were about two times larger than those between the yearly means. We performed a time series analysis for the more accurate HD 166014 minus HD 166093 differential BV magnitudes after spring 1992. The TSPA–method by Jetsu & Pelt (1999: hereafter Paper I) was applied separately to these B and V data. No periodicity between $1^{\rm d}$ and $100^{\rm d}$ was detected. Nor did we find indications of the $55^{\rm d}$ periodicity reported by Pavlovski et al. (1997) in their long-term UBV photometry of HD 166014.

Photometry of our K3II (Heard 1956) comparison star HD 166093 has been published only by Fernie (1983: $V = 7.21$ and $B = 8.56$). As for earlier studies of HD 166014 (o Her), our check star can be found in the photometric standard star catalogue by Perry et al. (1987), although luminosity variations were already suspected by Slettebak (1954) and Osawa (1959). This object was earlier classified as an eruptive variable by Kukarkin et al. (1971) and later as a Be-star of B9.5 III spectral type by Slettebak (1982). The published HD 166014 measurements by Johnson et al. (1966), Häggkvist & Oja (1966) and Pavlovski et al. (1997) agree in B, but range between 3.83 and 3.85 in V. The averages of the above values for HD 166014 are $V = 3.84$ and $B = 3.81$. We conclude that small irregular variability may be present in the comparison and/or check star, but this variability is insignificant ($\pm 0.^{\rm m}006$ in V) compared to that observed in V815 Her.

3. Analysis of the long-term photometry

3.1. The light curve modelling

The parameters of our second order ($K = 2$) light curve model

$$g(\bar{\beta}) = g(t, \bar{\beta}) = M + \sum_{\rm k=1}^{\rm K} B_{\rm k} \cos{(k2\pi ft)} + C_{\rm k} \sin{(k2\pi ft)}$$

were the mean (M), the amplitudes (B_1, B_2, C_1, C_2), and the frequency (f, i.e. the period $P = f^{-1}$). The free parameters were $\bar{\beta} = [M, B_1, B_2, C_1, C_2, f]$ or $\bar{\beta}_{\rm f} = [M, B_1, B_2, C_1, C_2]$ for a fixed f.

The long-term changes of the following five estimates were studied with this model: the mean (M), the total amplitude of the light curve (A), the primary and secondary minimum epochs in time ($t_{\rm min,1}, t_{\rm min,2}$) and the photometric rotation period (P). The total amplitude A is the difference between the global minimum and maximum of the model $g(t)$. The primary minimum $t_{\rm min,1}$ is the epoch for the global $g(t)$ minimum. If the model has another local $g(t)$ minimum, then $t_{\rm min,2}$ gives the epoch of this secondary minimum. The errors of all these five estimates were obtained with the bootstrap method (Paper I: Sect. 4).

The P, $t_{\rm min,1}$ and $t_{\rm min,2}$ estimates were determined by modelling the normalized magnitudes. These normalized magnitudes y (Paper I: Eq. 17) were derived within 92 subsets, where the number of observing nights in B or V was $N_{\rm B}$ or $N_{\rm V} \geq 8$, respectively. The frequency f was a free parameter in the *nonlinear* modelling of y, i.e. the free parameters were $\bar{\beta} = [M, B_1, B_2, C_1, C_2, f]$. This time series analysis was performed separately for each subset using the TSPA–method formulated in Paper I, where several detailed application examples can be found.

The $P \approx 1.8$ periodicity was detected in 90 subsets. But this periodicity was not among the five best ones in SET=37 and 42, even if the TSPA–method analysis was limited to the short period interval between 1.5 and 2.0 days. The obvious reason for not detecting the periodic rotational modulation in these two subsets was that the brightness of V815 Her remained nearly constant, e.g. the standard deviations in V were $0.^{\rm m}018$ (SET=37) and $0.^{\rm m}017$ (SET=42). The P, $t_{\rm min,1}$ and $t_{\rm min,2}$ estimates determined with the TSPA–method for the other 90 subsets are given in Table 3. The following three criteria formulated in Paper I were applied to reject some of these estimates:

> $R_{\rm I}$: The P, $t_{\rm min,1}$ and $t_{\rm min,2}$ estimates of a subset were rejected if the distribution of the model residuals or the distribution of the M, P, A, $t_{\rm min,1}$ or $t_{\rm min,2}$ bootstrap estimates was not gaussian.
> $R_{\rm II}$: The P, $t_{\rm min,1}$ and $t_{\rm min,2}$ estimates were rejected if the subset did not contain normalized magnitudes during at least 10 nights.
> $R_{\rm III}$: The $t_{\rm min,2}$ estimate of a subset was rejected if it was not present in at least 95% of the bootstrap models, i.e. such a $t_{\rm min,2}$ was considered "unreal".

The rejections with these criteria are indicated in Table 3.

The M and A estimates were determined from the modelling of the original B and V magnitudes. This *linear* B and V light curve modelling was performed with a fixed f using the subset ephemeris $\rm HJD_{min} = (t_{min,1} + P)E$ and the free parameters $\bar{\beta}_{\rm f} = [M, B_1, B_2, C_1, C_2]$. The mean and total amplitude of these light curves for subsets with $N_{\rm B}$ or $N_{\rm V} \geq 8$ are given in Table 3 ($M_{\rm B}, M_{\rm V}$, $A_{\rm B}$ and $A_{\rm V}$).

We studied the V815 Her light curves with a varying photometric rotation period, i.e. the best periodicity was determined for and applied in each subset. This approach was suitable for modelling both differential rotation and longitudinal shifts of activity centres. Because the "traditional" constant photometric period ephemeris was not applied, there was no unique phase for the whole data in our approach. Suitable phases for the whole data were searched for in the epochs of the phase dependent light curve features (i.e. $t_{\rm min,1}$ and $t_{\rm min,2}$). This unique series of time points has been analysed in Sect. 3.4.

3.2. The short- and long-term luminosity changes

Although the light curves of V815 Her frequently underwent significant changes even within a period of one month, continuous light curves could be obtained with a subset length of about $20^{\rm d}$ (Fig. 1). Hence the spot distribution did not evolve dramatically during ten rotations. Some V light curves had a

Table 3. The results for the subsets (SET): The photometric rotation period (P) and the epochs of the primary and secondary minima ($t_{\min,1}, t_{\min,2}$) were determined from the normalized magnitudes. The rejections of some P, $t_{\min,1}$ or $t_{\min,2}$ estimates with the $R_{\rm I}$, $R_{\rm II}$ or $R_{\rm III}$ criterion are denoted with "•". The mean ($M_{\rm B}, M_{\rm V}$) and the total amplitude ($A_{\rm B}, A_{\rm V}$) of the light curves were determined from the original B and V magnitudes with the subset ephemeris $\mathrm{HJD}_{\min} = (t_{\min,1} + P)\mathrm{E}$

	normalized magnitudes						original V and B magnitudes			
SET	P	$t_{\min,1}$	$t_{\min,2}$	$R_{\rm I}$	$R_{\rm II}$	$R_{\rm III}$	$M_{\rm V}$	$A_{\rm V}$	$M_{\rm B}$	$A_{\rm B}$
1	1.8069±0.0020	45971.247±0.100	...	...	•	...	0.5605±0.0033	0.140±0.017	−0.0893±0.0021	0.1233±0.0060
2	1.8059±0.0065	45996.801±0.058	...	...	...	...	0.5591±0.0026	0.0616±0.0075	−0.0788±0.0029	0.070±0.010
3	1.7919±0.0038	46108.457±0.026	46109.367±0.043	...	...	...	0.5736±0.0034	0.120±0.011	−0.0577±0.0023	0.1316±0.0064
4	1.8309±0.0048	46139.209±0.039	...	...	...	...	0.5755±0.0020	0.0946±0.0061	−0.0645±0.0031	0.1082±0.0098
5	1.834±0.015	46162.821±0.066	46161.87±0.12	...	...	•	0.5691±0.0029	0.0670±0.0083	−0.0613±0.0052	0.066±0.017
6	1.8228±0.0059	46185.115±0.030	46186.105±0.055	...	...	...	0.5715±0.0029	0.0544±0.0096	−0.0623±0.0025	0.0857±0.0082
7	1.7944±0.0027	46210.196±0.023	...	...	...	...	0.5703±0.0019	0.1151±0.0069	−0.0625±0.0022	0.1090±0.0080
8	1.8199±0.0044	46233.288±0.037	46234.019±0.042	...	...	...	0.5725±0.0035	0.109±0.016	−0.0614±0.0040	0.111±0.014
9	1.797±0.011	46271.576±0.053	46270.613±0.053	...	...	...	0.5623±0.0034	0.0660±0.0099	−0.0610±0.0027	0.0478±0.0082
10	1.8132±0.0082	46290.332±0.038	46291.295±0.035	...	...	...	0.5660±0.0020	0.0449±0.0078	−0.0652±0.0022	0.0489±0.0063
11	1.8091±0.0033	46313.998±0.029	...	...	...	...	0.5600±0.0016	0.0755±0.0053	−0.0756±0.0031	0.101±0.011
12	1.8002±0.0050	46339.667±0.039	46338.966±0.048	...	...	•	0.5316±0.0020	0.0605±0.0067	−0.0919±0.0016	0.0446±0.0054
13	1.817±0.018	46361.24±0.10	46362.30±0.11	...	...	•	0.5299±0.0035	0.067±0.013	−0.1023±0.0032	0.063±0.010
14	1.7910±0.0056	46551.967±0.071	46551.111±0.053	•	...	...	0.5046±0.0036	0.105±0.013	−0.1330±0.0060	0.111±0.020
15	1.839±0.012	46587.872±0.058	46586.910±0.083	...	...	...	0.5234±0.0020	0.0457±0.0061	−0.1198±0.0028	0.0465±0.0086
17	1.8070±0.0070	46858.731±0.017	...	•	•	...	0.4996±0.0037	0.135±0.011	−0.1463±0.0015	0.1574±0.0050
18	1.771±0.013	46888.313±0.098	46889.35±0.14	•	...	•	0.5008±0.0024	0.0469±0.0079	−0.1270±0.0036	0.050±0.012
19	1.8008±0.0083	46919.296±0.066	46920.200±0.068	•	•	...	0.5314±0.0041	0.0498±0.0099	−0.1009±0.0050	0.067±0.011
20	1.817±0.012	46962.82±0.12	...	...	...	...	0.5347±0.0034	0.0444±0.0089	−0.0920±0.0033	0.068±0.013
21	1.749±0.010	47069.884±0.083	...	•	...	...	0.5304±0.0016	0.0400±0.0052	−0.1003±0.0021	0.0464±0.0074
24	1.834±0.017	47277.744±0.050	...	...	...	...	0.4832±0.0036	0.0861±0.0081	−0.1637±0.0041	0.118±0.012
25	1.8065±0.0056	47297.668±0.026	47296.665±0.054	...	...	•	0.4736±0.0037	0.101±0.012	−0.1490±0.0026	0.1084±0.0087
26	1.822±0.023	47313.095±0.087	47313.899±0.100	...	...	...	0.4772±0.0041	0.032±0.013	−0.1611±0.0036	0.048±0.012
27	1.7978±0.0097	47418.19±0.12	47419.42±0.11	...	...	•	0.4511±0.0032	0.0552±0.0098	−0.1851±0.0021	0.0501±0.0068
28	1.806±0.010	47457.64±0.11	...	...	...	...	0.4518±0.0046	0.082±0.015	−0.1880±0.0047	0.089±0.016
29	1.830±0.023	47568.280±0.077	47568.949±0.063	•	•	•	0.4340±0.0041	0.077±0.018	...	...
30	1.8229±0.0082	47595.564±0.063	...	...	...	...	0.4325±0.0029	0.0476±0.0081	−0.2046±0.0023	0.0786±0.0074
31	1.8715±0.0095	47617.039±0.068	47617.732±0.061	...	...	...	0.4264±0.0031	0.0421±0.0076	−0.2123±0.0028	0.0483±0.0074
32	1.835±0.012	47637.388±0.099	...	...	...	...	0.4281±0.0031	0.067±0.011	−0.2179±0.0031	0.0566±0.0098
33	1.7980±0.0039	47659.616±0.023	47660.571±0.034	...	...	...	0.4302±0.0030	0.095±0.012	−0.2112±0.0030	0.068±0.011
34	1.8055±0.0092	47681.038±0.071	...	•	...	...	0.4333±0.0036	0.0886±0.0097	−0.2103±0.0035	0.068±0.011
35	1.813±0.015	47780.98±0.11	...	•	...	...	0.4510±0.0050	0.079±0.015	−0.2062±0.0039	0.082±0.015
36	1.827±0.028	47808.52±0.12	47809.37±0.11	...	...	...	...	...	−01899±0.0025	0.0403±0.0082
38	1.779±0.051	47927.07±0.15	47928.08±0.20	•	•	•	0.465±0.012	0.103±0.052	−0.1333±0.0090	0.102±0.029
39	1.815±0.019	47951.06±0.10	47951.90±0.11	•	...	...	0.442±0.011	0.128±0.047	−0.1487±0.0031	0.151±0.014
40	1.785±0.020	47989.420±0.090	47988.65±0.10	•	...	...	0.4690±0.0063	0.054±0.017	−0.1600±0.0038	0.078±0.011
41	1.808±0.011	48015.998±0.062	48016.896±0.075	...	...	...	0.4578±0.0045	0.054±0.015	−0.1730±0.0050	0.058±0.016
43	1.729±0.028	48178.83±0.12	48178.22±0.14	•	...	•	0.4853±0.0042	0.060±0.013	−0.1494±0.0056	0.058±0.026
45	1.8045±0.0078	48355.217±0.067	48354.615±0.079	...	...	•	0.5243±0.0044	0.078±0.013	−0.0974±0.0030	0.1138±0.0076
46	1.8267±0.0071	48376.605±0.049	...	...	...	...	0.5325±0.0026	0.1019±0.0079	−0.1067±0.0039	0.124±0.012
47	1.8098±0.0066	48398.479±0.054	...	...	...	...	0.5302±0.0028	0.1316±0.0091	−0.1004±0.0038	0.139±0.010
48	1.8134±0.0039	48420.279±0.049	...	...	...	...	0.5334±0.0049	0.132±0.017	−0.0963±0.0029	0.1609±0.0086
50	1.7648±0.0057	48723.41±0.13	...	•	...	...	0.5118±0.0023	0.0452±0.0069	−0.1169±0.0010	0.0613±0.0034
51	1.7950±0.0032	48746.237±0.021	...	...	...	...	0.5075±0.0027	0.0555±0.0068	−0.1243±0.0018	0.0829±0.0055
52	1.831±0.013	48793.123±0.076	48793.865±0.074	•	...	...	0.5053±0.0013	0.0177±0.0045	−0.1320±0.0013	0.0299±0.0048
53	1.7969±0.0048	48874.922±0.035	48875.834±0.051	...	...	...	0.4926±0.0019	0.0620±0.0058	−0.1421±0.0023	0.0831±0.0076
54	1.8100±0.0022	48899.970±0.028	...	...	...	...	0.4986±0.0011	0.0698±0.0035	−0.1377±0.0013	0.0956±0.0044
55	1.7869±0.0066	48928.653±0.040	48929.374±0.067	...	...	•	0.5025±0.0016	0.0402±0.0047	−0.1339±0.0022	0.0522±0.0058
57	1.791±0.010	49052.327±0.038	...	...	...	...	0.4894±0.0021	0.0694±0.0052	−0.1490±0.0016	0.0928±0.0048
58	1.8142±0.0023	49079.372±0.019	...	...	...	...	0.4944±0.0018	0.0713±0.0050	−0.1380±0.0015	0.0828±0.0044

Table 3. (continued)

	normalized magnitudes						original V and B magnitudes			
SET	P	$t_{\min,1}$	$t_{\min,2}$	$R_{\rm I}$	$R_{\rm II}$	$R_{\rm III}$	$M_{\rm V}$	$A_{\rm V}$	$M_{\rm B}$	$A_{\rm B}$
59	1.769±0.012	49102.82±0.10	...	•	...	...	0.4959±0.0018	0.0375±0.0059	−0.1401±0.0018	0.0391±0.0059
60	1.8190±0.0051	49125.842±0.031	49126.669±0.048	...	...	...	0.4946±0.0011	0.0425±0.0044	−0.1374±0.0017	0.0510±0.0063
61	1.8142±0.0049	49145.859±0.035	49146.796±0.071	...	...	•	0.4896±0.0017	0.0659±0.0045	−0.1410±0.0022	0.0764±0.0066
62	1.8071±0.0021	49236.478±0.061	...	...	...	...	0.4805±0.0017	0.1291±0.0060	−0.1542±0.0023	0.1494±0.0067
63	1.7295±0.0043	49285.729±0.029	49284.839±0.038	...	•	...	0.4769±0.0024	0.090±0.014	−0.1580±0.0021	0.090±0.010
64	1.7935±0.0031	49374.486±0.031	49375.236±0.035	...	...	•	0.4867±0.0014	0.0966±0.0023	−0.1442±0.0036	0.1109±0.0066
65	1.7880±0.0016	49408.506±0.012	49407.485±0.031	...	...	...	0.4717±0.0014	0.1019±0.0042	−0.1697±0.0019	0.1345±0.0057
66	1.8088±0.0031	49441.421±0.018	49440.626±0.025	...	...	...	0.4770±0.0017	0.0676±0.0069	−0.1624±0.0029	0.0837±0.0099
67	1.7898±0.0018	49465.561±0.013	49464.888±0.024	...	...	...	0.4878±0.0014	0.0799±0.0049	−0.1473±0.0012	0.0970±0.0049
68	1.7819±0.0029	49492.480±0.030	49493.395±0.033	...	...	...	0.4932±0.0020	0.0573±0.0070	−0.1386±0.0018	0.0615±0.0055
69	1.7982±0.0049	49528.005±0.036	49527.227±0.048	...	...	...	0.4897±0.0019	0.0516±0.0065	−0.1440±0.0024	0.0733±0.0075
70	1.826±0.011	49639.472±0.074	49638.763±0.090	...	...	•	0.4839±0.0022	0.0432±0.0061	−0.1449±0.0031	0.0481±0.0084
71	1.8005±0.0064	49662.541±0.096	49663.106±0.056	...	•	•	0.4821±0.0013	0.0379±0.0035	−0.1532±0.0020	0.0543±0.0057
72	1.8090±0.0021	49748.255±0.017	49747.388±0.026	...	...	...	0.5175±0.0021	0.0847±0.0068	−0.1097±0.0028	0.1035±0.0085
73	1.7756±0.0091	49787.685±0.052	49786.829±0.060	...	...	...	0.4944±0.0013	0.0171±0.0045	−0.1408±0.0024	0.0339±0.0075
74	1.7878±0.0097	49816.216±0.040	49817.214±0.043	•	...	...	0.5092±0.0027	0.0598±0.0094	−0.1251±0.0029	0.075±0.012
75	1.8077±0.0042	49841.170±0.025	...	...	...	...	0.5228±0.0018	0.0942±0.0052	−0.1026±0.0026	0.1089±0.0088
76	1.8094±0.0031	49866.505±0.024	...	...	...	...	0.5354±0.0015	0.0880±0.0042	−0.0898±0.0026	0.0925±0.0072
77	1.7872±0.0050	49888.060±0.041	...	...	...	...	0.5365±0.0017	0.0601±0.0053	−0.0876±0.0019	0.0668±0.0067
78	1.7990±0.0038	49984.136±0.029	49983.237±0.041	...	...	...	0.5580±0.0021	0.0809±0.0073	−0.0616±0.0032	0.1005±0.0078
79	1.7945±0.0053	50007.530±0.027	...	...	...	...	0.5848±0.0022	0.0779±0.0063	−0.0315±0.0027	0.0860±0.0079
80	1.7872±0.0034	50029.762±0.022	50030.662±0.051	...	...	...	0.5933±0.0025	0.0791±0.0068	−0.0253±0.0028	0.096±0.011
81	1.8137±0.0083	50112.210±0.070	50112.625±0.067	...	...	•	0.5869±0.0031	0.099±0.012	−0.0283±0.0030	0.114±0.010
82	1.7771±0.0036	50150.170±0.038	...	...	...	...	0.5921±0.0030	0.083±0.010	−0.0259±0.0024	0.0992±0.0082
83	1.7984±0.0021	50182.182±0.021	...	...	...	...	0.5850±0.0022	0.1366±0.0068	−0.0308±0.0021	0.1503±0.0070
84	1.8042±0.0020	50209.157±0.019	...	...	...	...	0.5712±0.0029	0.1657±0.0091	−0.0509±0.0034	0.188±0.010
85	1.7872±0.0027	50236.233±0.029	...	...	...	...	0.5704±0.0024	0.0859±0.0082	−0.0513±0.0028	0.094±0.010
86	1.7903±0.0057	50393.442±0.054	...	...	...	...	0.5453±0.0036	0.097±0.011	−0.0775±0.0040	0.120±0.013
87	1.8055±0.0050	50482.847±0.051	...	...	...	...	0.5438±0.0019	0.0818±0.0053	−0.0779±0.0024	0.0837±0.0068
88	1.8400±0.0077	50512.375±0.073	...	...	...	...	0.5315±0.0024	0.0459±0.0079	−0.0916±0.0030	0.0510±0.0096
89	1.8230±0.0058	50541.686±0.037	...	...	...	...	0.5357±0.0018	0.1083±0.0050	−0.0796±0.0030	0.1183±0.0077
90	1.7983±0.0041	50563.496±0.037	...	...	...	...	0.5413±0.0028	0.0982±0.0070	−0.0801±0.0022	0.1205±0.0062
91	1.7912±0.0022	50592.190±0.032	50591.644±0.050	...	...	•	0.5409±0.0016	0.0698±0.0040	−0.0800±0.0017	0.0849±0.0045
92	1.7612±0.0060	50620.329±0.039	...	...	...	...	0.5422±0.0019	0.0498±0.0063	−0.0761±0.0025	0.0650±0.0083
93	1.7763±0.0023	50712.112±0.043	...	...	...	...	0.5612±0.0016	0.0650±0.0051	−0.0498±0.0016	0.0750±0.0048
94	1.8004±0.0032	50746.131±0.062	...	...	...	...	0.5489±0.0014	0.0386±0.0036	−0.0661±0.0017	0.0528±0.0056
95	1.8216±0.0028	50830.059±0.017	50829.174±0.033	...	...	...	0.5278±0.0026	0.0725±0.0082	−0.1025±0.0013	0.0909±0.0052
96	1.878±0.010	50869.768±0.048	50868.642±0.048	...	...	•	0.5050±0.0018	0.0626±0.0064	−0.1182±0.0027	0.0664±0.0089
97	1.8297±0.0068	50894.439±0.081	50893.853±0.089	...	...	•	0.5398±0.0022	0.0355±0.0064	−0.0790±0.0024	0.0348±0.0082
98	1.7893±0.0035	50927.141±0.030	...	...	...	...	0.5326±0.0033	0.1068±0.0086	−0.0904±0.0037	0.120±0.012

nearly constant brightness level (e.g. SET=52 or 73). But there were numerous higher amplitude light curves, where the maximum brightness (e.g. SET=62), or almost the whole light curve (e.g. SET 33), exceeded these levels of constant brightness. It is therefore evident that there were starpots on the surface of V815 Her even during these periods of constant brightness.

The mean and the total amplitude of the light curve provided more detailed information of the long-term luminosity changes in V815 Her (Fig. 2: $M_{\rm B}$, $M_{\rm V}$, $A_{\rm B}$, $A_{\rm V}$). While the changes of the mean brightness were continuous, they revealed no signs of a regular spot cycle with a fixed period. Our TSPA-method time series analysis of these mean brightness changes did not detect any significant periodicities. For example, the approximately four year time difference between the two $M_{\rm V}$ maxima during 1989 and 1993 could not represent a regular activity cycle, because there was a deep $M_{\rm V}$ minimum at 1985. The correlation between the mean brightness and the colour index $M_{\rm B} - M_{\rm V}$ confirmed that V815 Her is hotter when brighter. Finally, the rapid changes of the total amplitudes $A_{\rm B}$ and $A_{\rm V}$ were more irregular than those of the mean, and certainly betrayed no signs of an activity cycle.

The M and A changes of V815 Her were not periodic, but unpredictable. The $\sim 15\%$ luminosity changes of V815 Her at visual wavelengths are about 100 times larger than those ob-

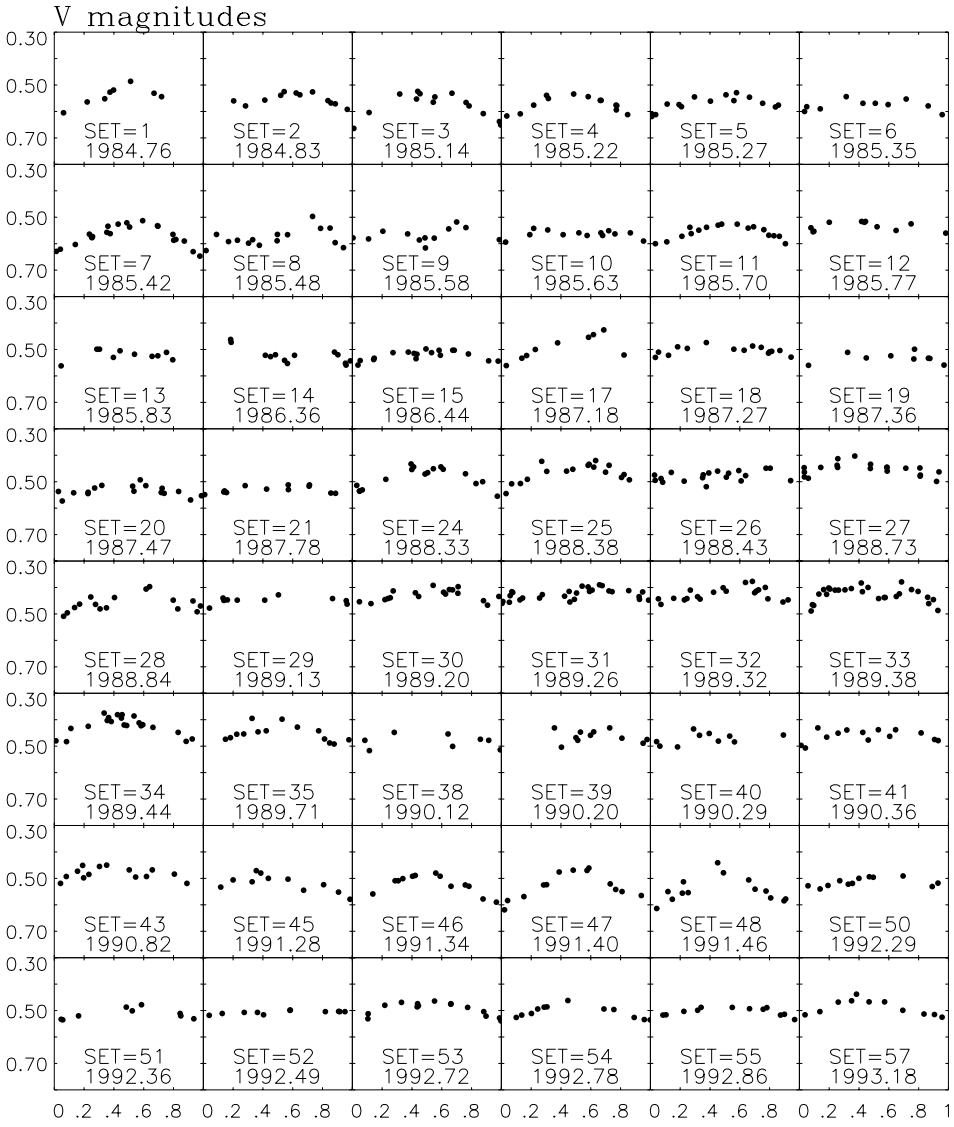

Fig. 1. The differential V magnitude light curves V815 Her minus HD 166093 for the $N_{\rm V} \geq 8$ subsets with the ephemerides $\mathrm{HJD}_{\rm min} = (t_{\rm min,1} + P)\mathrm{E}$ from Table 3. Note that no periodicity was detected in SET=37 and 42, while SET=36 had $N_{\rm V} = 7$. All differential V magnitudes from Table 1 are shown in Fig. 2a

served in the solar luminosity during one cycle (e.g. Willson & Hudson 1991: $\pm 0.1\%$). Yet the activity level changes in this G5V star may resemble those observed in the Sun (G2V) after-all. For example, the number of sunspots varies considerably from one cycle to another, the solar cycle period is not constant ($8^{\rm y} \lesssim P_{\rm cycle} \lesssim 15^{\rm y}$) and the solar activity may even fade for prolonged intervals, such as the Maunder Minimum (Eddy 1977; Baliunas & Vaughan 1985). Similar results have been obtained from a quarter of a century of CaII H&K emission line measurements for about one hundred solar-type stars. Baliunas et al. (1995) detected activity cycles in about 50% of the objects in this sample, but only 15% rated "good" or "excellent". Ossendrijver (1997) studied these best $P_{\rm cycle}$ in the context of dynamo theory, and made the following remark: "There are no stars with well-defined periods shorter than 7 years." In other words, not a single object has repeated more than three similar cycles during $25^{\rm y}$. A simple stellar analogy with the solar cycle would explain this result. Suppose the solar $P_{\rm cycle}$ were constant, but like for several centuries, the number of sunspots would vary considerably between different cycles. Were this the case for some active star with a constant $P_{\rm cycle}$, the shape of the M curve would be different during each cycle. Thus the power spectrum that relies on a sinusoidal model (e.g. Baliunas et al. 1995), or any other parametric period finding method, would fail in modelling these M changes, because the statistical significance of the $P_{\rm cycle}$ periodicity would be low. Furthermore, this stellar analogy of ours is quite optimistic, because $P_{\rm cycle} \neq \mathrm{constant}$ in the Sun. But if this analogy is sensible, the ratings "good" or "excellent" for $P_{\rm cycle} \geq 7^{\rm y}$ will steadily decrease from 15% when new observations are appended to those already analysed in Baliunas et al. (1995). Perhaps a sequence of more than three regular cycles is an extremely rare event in any active star. Considering the centuries of sunspot data, the CaII H&K sample in Baliunas et al. (1995), our results for V815 Her, and numerous similar photometric studies for other chromospherically active stars, it should be emphasized that the quasiperiodic nature of the starspot cycles prevents predictability. Some nonparametric methods assume no periodicity, but do uncover the different

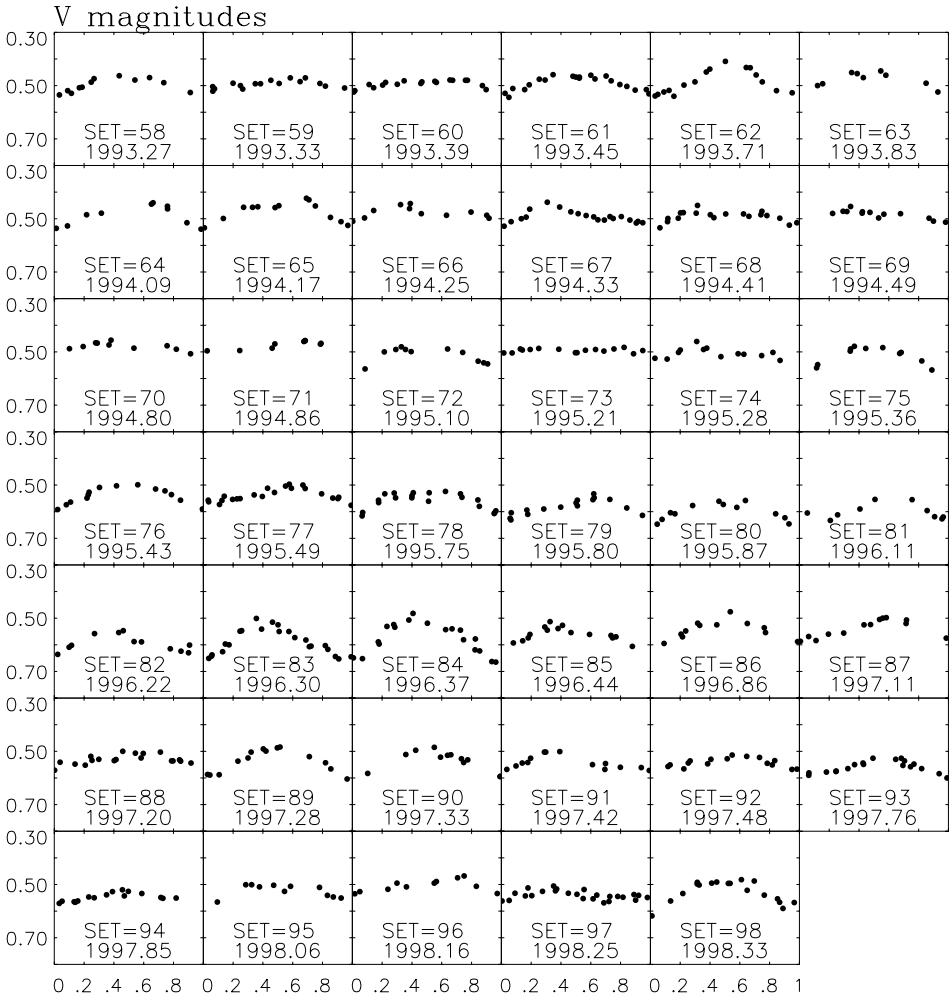

Fig. 1. (continued)

time scales of the starspot phenomena (e.g. Donahue et al. 1997: pooled variance). The results obtained with such methods may represent the maximum predictability that can be achieved in studies of starspot cycles. Afterall, we can not even predict the exact epoch for the maximum of the currently ongoing 23rd sunspot cycle (e.g. Li 1997).

3.3. The surface differential rotation

The photometric rotation periods of V815 Her are shown in Fig. 3, where the open and filled squares denote the P estimates rejected and not rejected with the $R_{\rm I}$ and $R_{\rm II}$ criteria (see Table 3). For these two $P_{\rm i} \pm \sigma_{\rm P_i}$ samples, we calculated the weighted mean $P_{\rm w} = (\sum w_{\rm i} P_{\rm i})/(\sum w_{\rm i})$ and its error $\Delta P_{\rm w} = \{[\sum w_{\rm i}(P_{\rm i} - P_{\rm w})^2]/[\sum w_{\rm i}]\}^{1/2}$, where $w_{\rm i} = \sigma_{\rm P_i}^{-2}$. As in Jetsu et al. (1993: Eq. 3), the dimensionless parameter $Z = 6\Delta P_{\rm w}/P_{\rm w}$ was adopted as the $\pm 3\Delta P_{\rm w}$ upper limit for the period changes around their mean $P_{\rm w}$. The less reliable P estimates gave $P_{\rm w} \pm \Delta P_{\rm w} = 1.792 \pm 0.027$ equal to $Z = 0.089 \equiv 8.9\%$. The changes of the reliable P were about two times smaller, $P_{\rm w} \pm \Delta P_{\rm w} = 1.800 \pm 0.014$, corresponding to $Z = 0.046 \equiv 4.6\%$. This confirmed that the $R_{\rm I}$ and $R_{\rm II}$ criteria from Paper I, which were also applied here, succeeded in rejecting the less reliable models. The presence of surface differential rotation was ascertained, because the $n = 71$ reliable P gave $\chi^2 = 961$, i.e. the hypothesis that "the photometric period is $P_{\rm w} = 1.800 \equiv$ constant" must definitely be rejected. But these P varied extremely rapidly and irregularly, e.g. for several successive subsets, the $\pm 3\sigma_{\rm P}$ error limits did not even overlap (Fig. 3: filled squares).

Our $Z \equiv 4.6\%$ for V815 Her was comparable to the earlier results obtained with the TSPA–method. The respective Z values were 7.5% for the G5III-IV FK Comae type star V 1794 Cyg (Jetsu et al. 1999: hereafter Paper II) and 3.3% for the K1V post T Tauri star V 368 Cep (Kahanpää et al. 1999). These Z values can be compared to the results obtained for a larger sample in Hall & Busby (1990: their Table 1). Their approach was based on the law of solar surface differential rotation, $P(b) = P_{\rm eq}/(1 - k\,\sin^2 b)$, where b, $P_{\rm eq}$ and k are the latitude, the equatorial rotation period and the differential rotation coefficient, respectively. The unknown $P_{\rm eq}$ was fixed to the orbital period $P_{\rm orb}$ in binary systems and to the mean of all observed $P_{\rm phot}$ in single stars. It was then assumed that the latitudinal range of starspot formation was confined between $b_{\rm max}$ and $b_{\rm min}$. These limits were used to calculate a parameter $h = \sin^2(b_{\rm max}) - \sin^2(b_{\rm min})$. For a fixed h, the differential

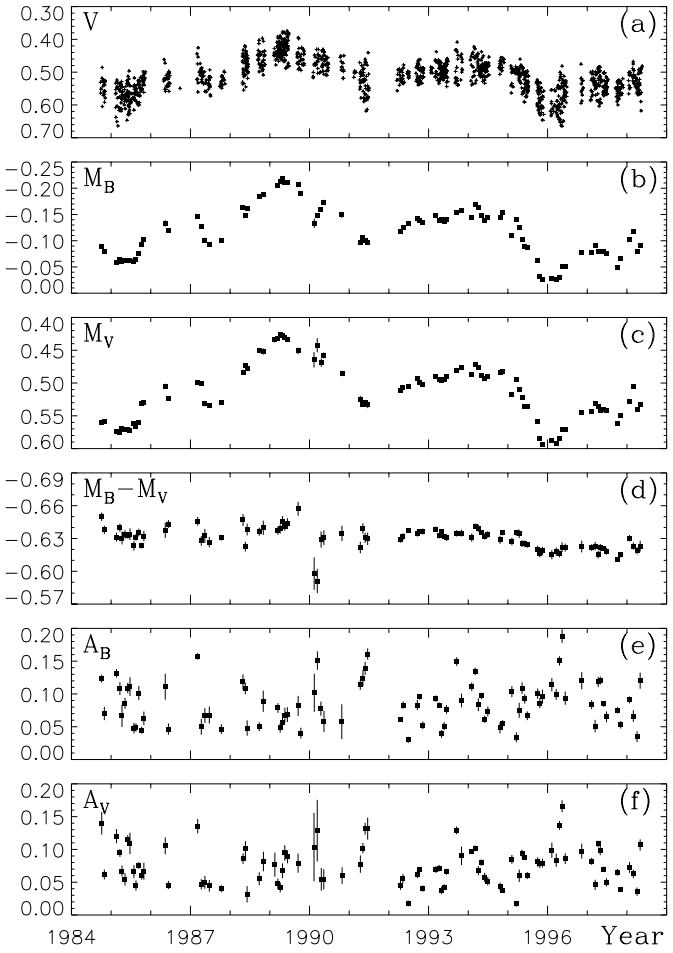

Fig. 2. a All $n = 1349$ differential V magnitudes V815 Her minus HD 166093 from Table 1. **b–f** The values of $M_{\rm B}$, $M_{\rm V}$, $M_{\rm B}-M_{\rm V}$, $A_{\rm B}$ and $A_{\rm V}$ from Table 3 ($\pm1\sigma$ errors)

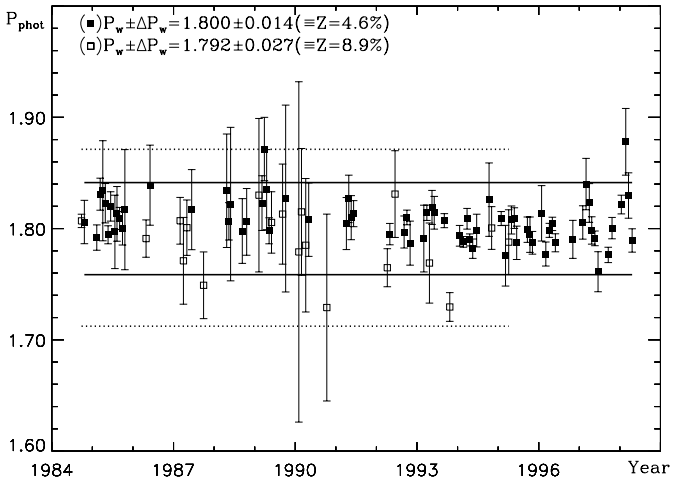

Fig. 3. The P estimates rejected ($n=19$ open squares) and not rejected ($n=71$ filled squares) with $R_{\rm I}$ and $R_{\rm II}$ (Table 3: $\pm3\sigma_{\rm P}$ errors!). The dotted and continuous horizontal lines denote the respective $P_{\rm w} \pm 3\Delta P_{\rm w}$ limits

rotation coefficient was then estimated from $k = \Delta P/(hP_{\rm eq})$, where $\Delta P = P(b_{\rm max}) - P(b_{\rm min})$. The largest and smallest values of all observed photometric rotation periods in any particular star were chosen to represent $P(b_{\rm max})$ and $P(b_{\rm min})$, respectively. Thus the stellar differential rotation coefficients in Hall & Busby (1990) can be compared to our Z with the relation $k \approx Z/h$, because the weighted mean $P_{\rm w}$ and its error $\Delta P_{\rm w}$ can be approximated with the relations $P_{\rm w} \cong P_{\rm eq}$ and $6\Delta P_{\rm w} \cong \Delta P$. For example, the extremes of the reliable P estimates for V815 Her would give $\Delta P = 0.117$, which is slightly larger than our $6\Delta P_{\rm w} = 0.084$. This "methodological" difference can be attributed to the statistical fluctuations of P, because the *two* extremes of P determine ΔP, while *all* P estimates are used in computing the error $\Delta P_{\rm w}$ of the weighted mean. The $\Delta P/P_{\rm eq}$ for the 15 stars in Hall & Busby (1990) had a mean of 0.013. But only one of those values, $\Delta P/P_{\rm eq} = 0.105$ for BY Dra, exceeded our $Z = 0.046$ for V815 Her. The reason for this result may be that BY Dra had the largest number of observed P values in Hall & Busby (1990: $n = 14$ in their Table 1). Hence the full latitude, or equivalently P, range was probably covered in BY Dra. That has almost certainly been the case here, with V815 Her having $n = 71$ reliable P estimates. The high $\Delta P/P_{\rm eq}$ of BY Dra could also be due to the fact that the luminosity ratio is about 2 in this binary system, where both components are active (Kövári 1999). The assumption in Hall & Busby (1990) of the primary being solely responsible for the $P_{\rm phot}$ changes is therefore not valid, because the differential rotation rates of both components influence the observed light curve of BY Dra.

The sunspots with $b_{\rm min} = 0°$ and $b_{\rm max} = 30°$ have $h = 0.25$. Hall & Busby (1990) used the latitude range of $45°$ that gave $0.5 < h < 0.7$. They lowered these h limits when the full latitude range was not observed in some objects having less P estimates (see their Fig. 2). Hall (1991) applied this method to a larger sample of 85 stars. His main result was that surface differential rotation is weaker in the more rapidly rotating stars. Although V815 Her rotates extremely rapidly, the solar $h = 0.25$ and our $Z = 0.046$ here gives $k \approx Z/h = 0.184$ that nearly equals the solar $k = 0.189$ (Allen 1963). But this result is very sensitive to the chosen h, because a $\pm2°$ change in $b_{\rm max} = 30°$ would give $0.164 < k < 0.209$ for V815 Her.

If the law of solar differential rotation can be applied to other stars, the solar $h = 0.25$ will underestimate the stellar k for narrow latitudinal activity ranges, e.g. $b_{\rm min} = 70°$ and $b_{\rm max} = 80°$ equals $h = 0.09$. The determination of P is difficult for starspots located closer to the pole ($b_{\rm max} \sim 90°$). The starspot latitudes can not usually be uniquely modelled from the light curve (Eker 1999), while the Doppler imaging methods may solve this problem. But different imaging methods have also given conflicting results for the same object (e.g. Strassmeier 1996: V711 Tau in Table 1).

But even if the law of solar differential rotation were valid for other stars, it would not guarantee a one to one relation between the starspot latitude and the photometric rotation period. This is certainly not the case in the Sun, as emphasized by Howard (1994: see his Fig. 2). Furthermore, the younger sunspots rotate

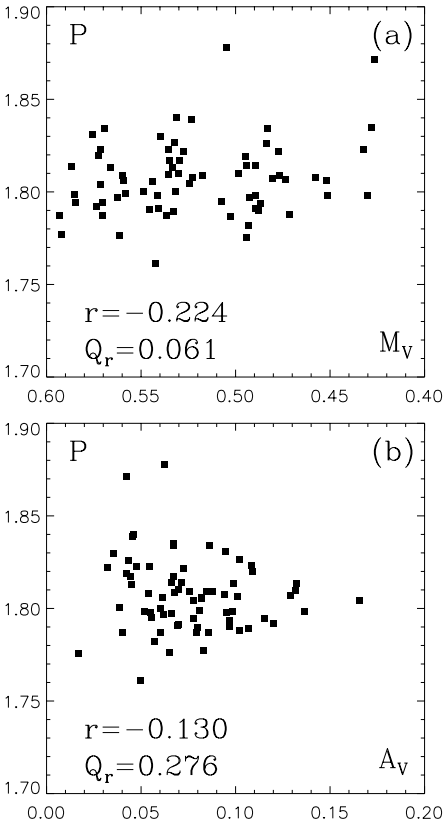

Fig. 4. a The linear correlation coefficient (r) and its significance ($Q_{\rm r}$) between the reliable P and the simultaneous $M_{\rm V}$ (Table 3: $n = 70$). **b** The reliable P and the simultaneous $A_{\rm V}$, otherwise as in **a**

faster than the older ones, and the surface differential rotation also changes within the solar cycle (e.g. Pulkkinen & Tuominen 1998). The rapid P changes of V815 Her in our Fig. 3 do not therefore necessarily contradict the solar-stellar connection.

It seemed that the surface rotation rate decreased when V815 Her became brighter, because the linear correlation coefficient $r = -0.224$ between the reliable P and and the simultaneous $M_{\rm V}$ had a significance of $Q = 0.061$ (Fig. 4a). If the higher brightness levels were connected to higher spot latitudes, this result would indicate solar-type surface differential rotation in V815 Her. The negative $r = -0.130$ value for the correlation between P and $A_{\rm V}$ did support this projection effect, but only with a very low $Q_{\rm r} = 0.276$ significance (Fig. 4b).

The results in Figs. 3 and 4 were related to the short-term seasonal P changes. Considering the latitudinal migration of sunspots during the solar cycle, one might expect some connection between the yearly mean periodicity and brightness in other chromospherically active stars. An earlier TSPA–method analysis revealed surprisingly regular yearly periodicity changes in V 1794 Cyg that qualitatively resembled the solar butterfly diagram (Paper II: Fig. 7). This type of analysis was also performed for all normalized magnitudes of V815 Her during each year. The periodicities $P_{\rm Y1}$ obtained from $n_{\rm SET,1}$ subsets are given in Table 4. The $P_{\rm Y1}$ changes of V815 Her were extremely irregular around $P_{\rm w} \pm \Delta P_{\rm w} = 1.799 \pm 0.013$ corresponding to

Table 4. The periodicities $P_{\rm Y1}$ determined with the TSPA-method from $n_{\rm SET,1}$ subsets of normalized magnitudes during each year. The yearly mean periodicities $P_{\rm Y2}$ calculated from the $n_{\rm SET,2}$ reliable P values in Table 3

Year	$n_{\rm SET,1}$	$P_{\rm Y1}$	$n_{\rm SET,2}$	$P_{\rm Y2}$
1984	2	1.8188±0.0028	...	...
1985	11	1.81947±0.00037	11	1.812±0.015
1986	2	1.8207±0.0033	...	...
1987	5	1.82823±0.00079	...	...
1988	5	1.79842±0.00042	5	1.813±0.015
1989	9	1.81723±0.00057	5	1.830±0.027
1990	6	1.7853±0.0049	...	...
1991	4	1.81528±0.00085	4	1.8136±0.0095
1992	6	1.78586±0.00037	4	1.7972±0.0096
1993	7	1.80766±0.00030	5	1.809±0.011
1994	8	1.78391±0.00027	7	1.798±0.015
1995	9	1.81298±0.00034	8	1.796±0.012
1996	6	1.79039±0.00024	6	1.795±0.013
1997	8	1.79084±0.00027	8	1.799±0.025
1998	4	1.8266±0.0010	4	1.830±0.037

$Z = 0.044$ (Fig. 5a). The dispersion of these yearly $P_{\rm Y1}$ was of the same order as that of the short-term P during individual subsets (Fig. 3). The constant period ($P_{\rm w} = 1.799$) hypothesis gave $\chi^2 = 15772$ for $n = 15$ values, indicating that these $P_{\rm Y1}$ were certainly variable. But there were also longer time intervals when the $P_{\rm Y1}$ level remained nearly constant, e.g. from 1984 to 1987, or from 1996 to 1997. Obviously, the $P_{\rm Y1}$ changes did not correlate with the yearly mean brightness M of V815 Her.

As an alternative approach, we calculated the averages $P_{\rm Y2}$ for all $n_{\rm SET,2}$ reliable P estimates during each year (Table 4). No $P_{\rm Y2}$ was obtained for the years 1984, 1986, 1987 and 1990, having less than two reliable P estimates in Table 3. The $P_{\rm Y2}$ had the weighted mean $P_{\rm w} \pm \Delta P_{\rm w} = 1.805 \pm 0.009$ equal to $Z = 0.030$ (Fig. 5b). The interesting result was that these $P_{\rm Y2}$ fit the hypothesis of constant period (i.e. $P_{\rm w} = 1.805$), because the $\chi^2 = 4.9$ for $n = 11$ had a significance of 0.90. In other words, this yearly averaging erased the periodicity changes completely. It was therefore useless to search for correlations, e.g. between the yearly $P_{\rm Y2}$ and M of V815 Her. This result also implied that the seasonal P within a single year may sometimes cover the full range of periodicity changes in V815 Her, as already indicated by Fig. 3.

3.4. The active longitudes

Observational evidence for the existence of a sector structure at the surface of chromospherically active stars was already presented about two decades ago (e.g. Eaton & Hall 1979). In several cases, the formation of starspots seems to concentrate on two long-lived active longitudes rotating with a constant angular velocity and maintaining an angular separation of about $180°$ (e.g. Hall 1987, 1991; Jetsu et al. 1993; Berdyugina & Tuominen 1998). Detections of similar structures in the Sun have also been reported (e.g. Bai 1988; Jetsu et al. 1997). The obvious

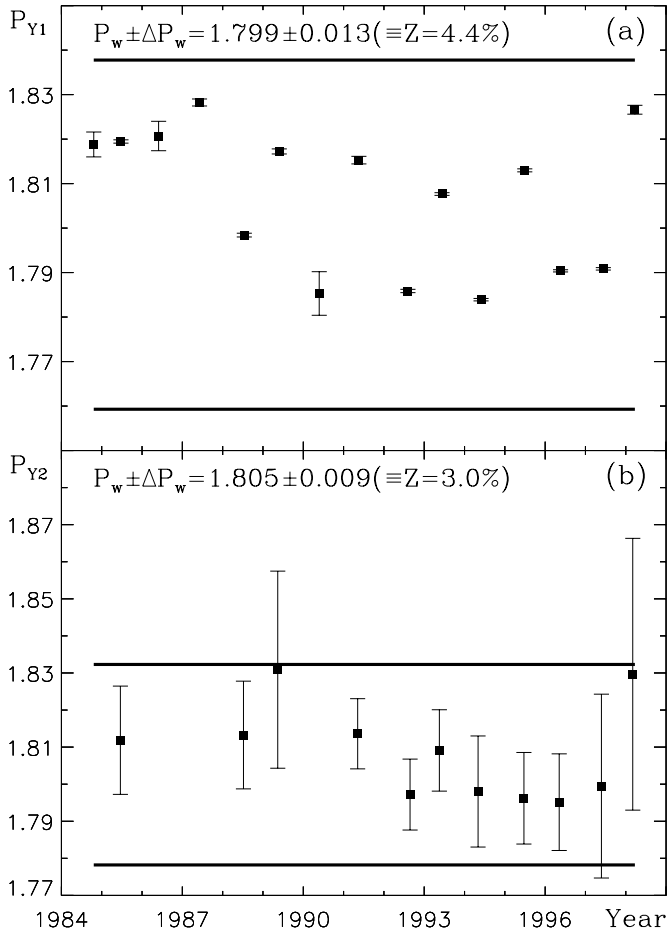

Fig. 5a and b. The yearly $P_{\rm Y1}$ and $P_{\rm Y2}$ (Table 4: $\pm1\sigma$ errors)

geometrical interpretation of the stellar light curve has been that the primary minimum ($t_{\rm min,1}$) represents the epoch when the region of *stronger* activity crosses the visible stellar disk. The secondary minimum ($t_{\rm min,2}$), if present, would then have been caused by another *weaker* region of activity. For example, active longitudes were detected in four RS CVn systems by Jetsu (1996), who analysed the primary and secondary minimum epochs determined by Henry et al. (1995b). The most recent similar analysis was performed for V 1794 Cygni in Paper II.

Our search for active longitudes in V815 Her began by using the $R_{\rm I}$, $R_{\rm II}$ and $R_{\rm III}$ rejection criteria to separate the primary and secondary minima from Table 3 into two groups.

> Group $T_{\rm A}$: The $n_1 = 94$ reliable $t_{\rm min,1}$ and $t_{\rm min,2}$ estimates, which were *not* rejected with $R_{\rm I}$, $R_{\rm II}$ or $R_{\rm III}$.
> Group $T_{\rm B}$: The $n_2 = 45$ less reliable $t_{\rm min,1}$ and $t_{\rm min,2}$ estimates, which were *rejected* with $R_{\rm I}$, $R_{\rm II}$ or $R_{\rm III}$.

Both series of time points represent circular data when folded with an arbitrary period P. Several tests for analysing circular data have been described, e.g. in Batshelet (1981) or Jetsu & Pelt (1996: hereafter Paper III). We applied the nonparametric Kuiper (1960: K-method) and the Swanepoel & De Beer (1990: SD-method) tests to search for periodicity in the $T_{\rm A}$ epochs. Since both methods have been thoroughly described in Paper III, the same notations are also used here. These methods were used to test the hypothesis (H_0) that "*the phases of $T_{\rm A}$ with an arbitrary period P are randomly distributed between 0 and 1.*" The preassigned significance level for rejecting H_0 was fixed to $\gamma_0 = 0.001$. The tested period interval was between 1.7 and 1.9 days, because all seasonal P were within $\pm5\%$ around $1.^{\rm d}8$.

The $T_{\rm A}$ epochs were sparsely distributed. Their time span of 4930 days covered about 2739 rotations for periodicities close to 1.8 days, i.e. the mean separation between consecutive $T_{\rm A}$ was approximately 29 rotations. It was therefore difficult to determine the precise number of tested independent frequencies (m). The critical levels, $Q_{\rm SD}$ and $Q_{\rm K}$, for the periods detected with the SD- and K-methods were calculated from $m = 305$ (Paper III: Eq. 13). We did not apply the weighted versions of the SD- and K-methods that could also utilize the weights $w_{\rm T_A} = \sigma_{\rm T_A}^{-2}$ (Paper III: WK- and WSD-methods). Apart from the inaccurate m value, the scatter of $w_{\rm T_A}$ introduced additional complications. Several useful parameters for describing the quality of a weighted series of time points were introduced in Jetsu (1996). For the $w_{\rm T_A}$ weights of V815 Her, the most relevant values of these descriptive parameters were the ratio $W_{\rm R} = \max\{w_{\rm T_A}\}/\min\{w_{\rm T_A}\} = 100$ and the SD-method statistics "breakdown" parameter $R(s) = 0.05$. This data quality, and the large $m = 305$ value, prevented reliable WSD- or WK-method significance estimates.

The critical level of the best period detected with the K-method, $P_{\rm K} = 1.79081 \pm 0.00030$, was only $Q_{\rm K} = 0.94$. The number of independent frequencies, m', indicated by the empirical $r(k)$ correlation function (Paper III: Eq. 14) of the K-method periodogram exceeded $m = 305$. Hence the above $Q_{\rm K}$ overestimated the significance of $P_{\rm K}$, and we could safely conclude that the K-method detected no significant periodicity in the $T_{\rm A}$ epochs. The SD-method detected one period reaching $\gamma_0 = 0.001$. This periodicity of $P_{\rm SD} = 1.79244 \pm 0.00034$ had $Q_{\rm SD} = 0.00041$. The m' estimate obtained from the empirical $r(k)$ function of the SD-method periodogram was at least three times larger than $m = 305$. But even if m were adjusted to $m' = 3m$ or $4m$, the critical level would increase from $Q_{\rm SD} = 0.00041$ only to 0.0012 or 0.0016, respectively (Paper III: Eq. 19). Thus the $P_{\rm SD} = 1.79244$ periodicity is very significant, although we could not reject H_0 with $\gamma_0 = 0.001$, because the precise m value was uncertain.

The $P_{\rm SD}$ and $P_{\rm K}$ periodicities were obtained from the $T_{\rm A}$ epochs. Because the $T_{\rm B}$ epochs were not analysed, they offered an opportunity to compare the predictivity of $P_{\rm SD}$ and $P_{\rm K}$. The phase distributions of $T_{\rm A}$ and $T_{\rm B}$ should be similar for "real" periodicity. The two sample method by Kuiper (1960: K2-method) was applied to test the hypothesis (H_1) that "*the phase distributions of $T_{\rm A}$ and $T_{\rm B}$ represent random samples drawn from the same distribution*". Under H_1, the critical levels of $P_{\rm SD}$ and $P_{\rm K}$ with the nonweighted K2-method were $Q_{\rm K2} = 0.33$ and 0.066 (Paper III: Eq. 27). Had the preassigned significance level for rejecting H_1 been fixed to $\gamma_1 = 0.001$, this result would have been inconclusive. Nevertheless, this test with the K2-method did

confirm that the $T_{\rm B}$ and $T_{\rm A}$ phase distributions were more similar with $P_{\rm SD}$ than $P_{\rm K}$.

The primary and secondary minimum phases of $T_{\rm A}$ and $T_{\rm B}$ with $P_{\rm SD}$ are displayed in Fig. 6. The arbitrary zero phase epoch (t_0) is the first $t_{\min,1}$ in Table 3, because the results with the SD- and K-methods are independent of the chosen t_0. Considering the presence of strong surface differential rotation, the observed rapid changes in these phases were no surprise, e.g. the reliable primary minima varied between 0.0 and 0.9 in phase during 1985 (Fig. 6a: filled squares). The distribution of the $T_{\rm A}$ primary minima was unimodal and broad, and the superimposed $T_{\rm B}$ distribution was similar (Fig. 6b). Both secondary minimum distributions resembled a random distribution (Fig. 6c). The $P_{\rm SD}$ periodicity detection in $T_{\rm A}$ is connected to the dark combined distribution of the primary and secondary minima in Fig. 6d. The K2-method did confirm that the superimposed white $T_{\rm B}$ distribution resembles the dark one. Note that the dark distribution for the regions of *stronger* activity has remained more or less unimodal (Fig. 6b). The smaller peak in the dark combined distribution, which is located at about 0.5 in Fig. 6d, is due to the *weaker* regions of activity, i.e. the secondary minima from Fig. 6c. We conclude that one active longitude, which has rotated with a constant period of $P_{\rm SD} = 1.79244$ for about 14 years, may exist in V815 Her. Furthermore, if this structure is rotating pseudosynchronously, the ratio $S = P_{\rm orb}/P_{\rm SD} = 1.0097 \pm 0.0002$ would indicate an eccentricity of $e = \sqrt{(S-1)/6} = 0.0402 \pm 0.0004$ (Hut 1981: Eq. 43) that agrees with $e = 0.05 \pm 0.02$ obtained from spectroscopy (Dempsey et al. 1996).

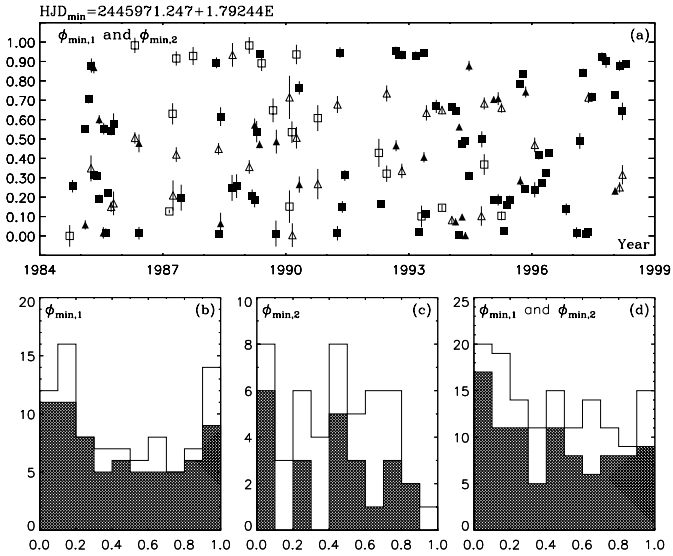

Fig. 6. a The phases of the primary and secondary minima with $\mathrm{HJD_{min}} = 2445971.247 + 1.79244\mathrm{E}$: $\phi_{\min,1}$ (filled squares $\equiv T_{\rm A}$; open squares $\equiv T_{\rm B}$) and $\phi_{\min,2}$ (filled triangles $\equiv T_{\rm A}$; open triangles $\equiv T_{\rm B}$) **b** The $\phi_{\min,1}$ distribution (dark$\equiv T_{\rm A}$; white$\equiv T_{\rm B}$) **c** The $\phi_{\min,2}$ distribution (dark$\equiv T_{\rm A}$; white$\equiv T_{\rm B}$) **d** The combined $\phi_{\min,1}$ and $\phi_{\min,2}$ distributions

4. Conclusions

We have performed the time series analysis of the long-term photometry of the RS CVn system V815 Her, where the starspots on the surface of the primary cause the observed luminosity variation. The G5V spectral-type of this primary is quite close to that of the Sun (G2V). If $P_{\rm phot} = 1.^{\rm d}8$ is compared to the solar equatorial rotation period of $25^{\rm d}$, V815 Her rotates very rapidly. The tidal forces in this system have nearly synchronized the orbital and rotation periods, and hence its $v \sin i = 31.2$ km s^{-1} (Fekel 1997) exceeds the typical values in other G-type main-sequence stars (Gray 1982). The observed magnetic activity in V815 Her is strong, as would be predicted by rotation-activity relations (e.g. Strassmeier et al. 1990; Hall 1991; Böhm-Vitense 1992). Among these indicators of strong activity are the large starspot-induced rotational and long-term luminosity changes, about 15% at the visual wavelengths. The weaker solar magnetic activity causes luminosity changes of $\pm 0.1\%$ (e.g. Willson & Hudson 1991).

Each seasonal light curve of V815 Her was modelled with a variable photometric rotation period, which was determined with the TSPA–method from the normalized magnitudes (Sect. 3.1). Unlike the traditional constant period ephemeris, this variable period approach enabled simultaneous modelling of surface *differential rotation* and *longitudinal activity* shifts. The former phenomenon was recorded by the P changes, and the latter by the $t_{\min,1}$ and $t_{\min,2}$ changes. The seasonal periodicities were then used in modelling the mean (M) and the total amplitude (A) of the contemporary B and V light curves (Fig. 1).

No regular cycle period ($P_{\rm cycle}$) was detected in the long-term M and A changes (Sect. 3.2: Fig. 2). But the slow and continuous M changes in V815 Her resembled, at least qualitatively, those observed in the Sun. The solar $P_{\rm cycle} \approx 11^{\rm y}$ has not been precise, but has varied between $8^{\rm y}$ and $15^{\rm y}$ (Eddy 1977). The number of sunspots has varied considerably from one cycle to another, not to mention the unpredictable prolonged activity suppressions, like the Maunder (1645–1715), Spörer (1420–1530), Wolf (1280–1340) or Oort (1010–1050) minima (Baliunas & Vaughan 1985). Thus the solar-stellar connection would not predict that the stellar activity cycles are regular. This might be the reason for not detecting significant cycle periodicities in activity related parameters, e.g. during observing intervals longer than $\sim 3P_{\rm cycle}$ (Baliunas et al. 1995). The parametric period finding methods can not simply detect a variable $P_{\rm cycle}$, nor adapt to the activity level differences between separate cycles. Yet, there will inevitably be cases when the time series analysis detects regularities in some activity related data from the *past*, but fails in predicting those of the *future*. For example, spots with a certain characteristic lifetime, but forming at random locations, can also produce long-term light curve changes that resemble an activity cycle (Eaton et al. 1996).

The rapid and irregular changes of the seasonal P confirmed the presence of surface differential rotation in V815 Her (Sect. 3.3: Fig. 3). Such irregularity does not contradict the solar-stellar connection, because the relation between the rotation period and the latitude of sunspots has been far from regular (Howard 1994: Fig. 2). An upper limit of $Z = 6\Delta P_{\rm w}/P_{\rm w} =$

$0.046 \equiv 4.6\%$ for these period changes was calculated from the weighted mean $P_{\rm w} \pm \Delta P_{\rm w}$ of all reliable P estimates. This Z value was high, when compared to the surface differential coefficients k obtained for a larger sample of stars in Hall & Busby (1990). We had almost certainly observed the full range of period changes in V815 Her, because the number of reliable P was $n = 71$. Hence two assumptions were made. Firstly, the latitudinal range of starspot formation in V815 Her has been the same as that of the sunspots. Secondly, the law of solar surface differential rotation could be applied in V815 Her. With these assumptions, V815 Her had $k = 0.184$, which was nearly equal to the solar $k = 0.189$ (Allen 1963). This result did not support the idea of surface differential rotation being weaker in rapidly rotating stars (Hall 1991). However, we emphasized that even if the law of solar differential rotation were valid in other stars, the results obtained for k are very sensitive to the assumed latitudinal range of the starspot formation. The observed rapid and irregular P changes could not be used to determine the law of differential rotation in V815 Her. Even if there were such a law, this irregularity could also be due to random changes in the latitude of maximum spottedness (see Eaton et al. 1996). The significance of the linear correlation between the reliable values of seasonal periodicities (P) and the mean brightness (M) was $Q_{\rm r} = 0.06$ (Fig. 4a). This result would support the presence of solar-type differential rotation in V815 Her, if higher brightness levels were connected to higher starspot latitudes. But we found no evidence for the regular solar-type latitudinal migration, because the yearly periodicities changed irregularly and did not correlate with the brightness level of V815 Her (Figs. 5a and b).

The primary and secondary minima of the seasonal light curves, $t_{\rm min,1}$ and $t_{\rm min,2}$, were used to search for active longitudes in V815 Her (Sect. 3.4). These epochs were divided into two groups, the reliable ($T_{\rm A}$) and the less reliable ($T_{\rm B}$) estimates. Both groups contained estimates of the primary and secondary minimum epochs. This allowed us to model the presence of two active longitudes on the surface of V815 Her during some seasons. Of the two nonparametric methods that were applied to $T_{\rm A}$, the SD-method detected the best periodicity of $P_{\rm SD} = 1.79244 \pm 0.00034$ between and 1.7 and 1.9 days. This periodicity reached the critical level $Q_{\rm SD} = 0.00041$. But with the preassigned significance level of $\gamma_0 = 0.001$, we could not reject the random distribution hypothesis H_0 for the phases of $T_{\rm A}$ with $P_{\rm SD}$, because the precise number of independent tested frequencies was uncertain. An additional test with the K2-method showed that the phase distributions of $T_{\rm A}$ and $T_{\rm B}$ were similar with the $P_{\rm SD}$ periodicity. All these results indicated that the regions of *stronger* activity on the surface of V815 Her have concentrated on *one* active longitude, which has rotated with a constant period of $P_{\rm SD} = 1.79244$ for about 14 years (Fig. 6). This would not support the idea presented by Eaton et al. (1996), because the presence of such a long-lived structure means that the spots in V815 Her are not formed at random locations. As for the solar-stellar connection, we refer to the similar structures reported in the Sun (e.g. Bai 1988; Jetsu et al. 1997).

Acknowledgements. The work by T.H. was supported by a grant from the Jenny and Antti Wihuri foundation, and by Helsinki University research funding for "Time Series Analysis of Stellar Magnetic Activity" (No.974/62/98). Astronomy with automated telescopes at Tennessee State University is supported through NASA grants NCC5–96 and NCC5–228, which funds TSU's Center for Automated Space Science, and NSF grant HRD–9706268, which funds TSU's Center for Systems Science Research. This research has made use of the Simbad-database operated at CDS, Strasbourg, France. We wish to thank our referee Dr. K. Olah for valuable comments on the manuscript.

References

Allen C.W., 1963, Astrophysical Quantities. Athlone Press, University of London
Bai T., 1988, ApJ 328, 860
Baliunas, S.L., Vaughan A.H., 1985, ARA&A 23, 379
Baliunas S.L., Donahue R.A., Soon W.H., et al., 1995, ApJ 438, 269
Barrado y Navascues D., Fernandez-Figueroa M.J., Garcia Lopez R.J., de Castro E., Cornide M., 1997, A&A 326, 780
Batschelet E., 1981, Circular Statistics in Biology. Academic Press, London
Berdyugina S.V., Tuominen I., 1998, A&A 336, L25
Bopp B.W., 1984, ApJS 54, 387
Böhm-Vitense E., 1992, AJ 103, 608
Dempsey R.C., Linsky J.L., Schmitt J.H.M.M., Fleming T.A., 1993a, ApJ 413, 333
Dempsey R.C., Linsky J.L., Fleming T.A., Schmitt J.H.M.M., 1993b, ApJS 86, 599
Dempsey R.C., Neff J.E., O'Neal D., Olah K., 1996, AJ 111, 1356
Donahue R.A., Dodson A.K., Baliunas S.L., 1997, Solar Phys. 171, 211
Drake S.A., Simon T., Linsky J.L., 1986, AJ 91, 1229
Drake S.A., Simon T., Linsky J.L., 1992, ApJS 82, 311
Eaton J.A., Hall D.S., 1979, ApJ 227, 907
Eaton J.A., Henry G.W., Fekel F.C., 1996, ApJ 462, 888
Eddy J.A., 1977, In: White O.R. (ed.) The Solar Output and Its Variation. Colorado Assoc. Univ. Press, Boulder, p. 51
Eggen O.J., 1978, IBVS 1426
Eker Z., 1999, ApJ 512, 386
Eker Z., Hall D.S., Anderson C.M., 1995, ApJS 96, 581
Fekel F.C., 1997, PASP 109, 514
Fekel F.C., Moffett T.J., Henry G.W., 1986, ApJS 60, 551
Fernandez-Figueroa M.J., Montesinos B., de Castro E., et al., 1986, A&A 169, 219
Fernie J.D., 1983, ApJS 52, 7
Gray D.F., 1982, ApJ 261, 259
Gunn A.G., Spencer R.E., Abdul Aziz H., et al., 1994, A&A 291, 847
Häggkvist L., Oja T., 1966, Arkiv för Astron. 4, 137
Hall D.S., 1987, Publ. Astr. Inst. Czechoslovakia 70, 77
Hall D.S., 1991, In: Tuominen I., Moss D., Rüdiger G. (eds.) The Sun and Cool Stars: activity, magnetism, dynamos. IAU Coll. 130, Springer-Verlag, Heidelberg, p. 353
Hall D.S., Busby M.R., 1990, In: Ibanoğlu C. (ed.) Active Close Binaries. Kluwer, Dordrecht, p. 377
Heard J.F., 1956, Publ. David Dunlap Obs. 2, 107
Henry G.W., 1995a, In: Henry G.W., Eaton J.A. (eds.) Robotic Telescopes: Current Capabilities, Present Developments, and Future Prospects for Automated Astronomy. PASPC 79, p. 37
Henry G.W., 1995b, In: Henry G.W., Eaton J.A. (eds.) Robotic Telescopes: Current Capabilities, Present Developments, and Future Prospects for Automated Astronomy. PASPC 79, p. 44

Henry G.W., Newsom M.S., 1996, PASP 108, 242
Henry G.W., Fekel F.C., Hall D.S., 1995a, AJ 110, 2926
Henry G.W., Eaton J.A., Hamer J., Hall D.S., 1995b, ApJS 97, 513
Howard R.F., 1994, In: Balasubramaniam K.S., Simon G.W. (eds.) Solar Active Region Evolution: Comparing Models with Observations. PASPC 68, p. 1
Hut P., 1981, A&A 99, 126
Jetsu L., 1996, A&A 314, 153
Jetsu L., Pelt J., 1996, A&AS 118, 587 (Paper III)
Jetsu L., Pelt J., 1999, A&AS 139, 629 (Paper I)
Jetsu L., Pelt J., Tuominen I., 1993, A&A 278, 449
Jetsu L., Pohjolainen S., Pelt J., Tuominen I., 1997, A&A 318, 293
Jetsu L., Pelt J., Tuominen I., 1999, A&A 351, 212 (Paper II)
Johnson H.L., Mitchell R.I., Iriarte B., Wisniewski W.Z., 1966, Comm. Lunar Plan. Lab. 4, 99
Kahanpää J., Jetsu L., Alha L., et al., 1999, A&A 350, 513
Kövári Zs., 1999, In: Butler C.J., Doyle J.G. (eds.) Solar and Stellar Activity: Similarities and Differences. PASPC 158, p 166
Kuiper N.H., 1960, Proc. Koningkl. Nederl. Akad. Van Wettenschappen, Series A 63, 38
Kukarkin B.V., Kholopov P.N., Pskovsky Yu.P., et al., 1971, General Catalogue of Variable Stars. 3rd Edition
Li Y., 1997, Solar Phys. 170, 437
Liu X.-F., Zhao G., Tan H.-S., Lu F.-J., 1993, Chin. Astron. Astrophys. 17, 51
Malina R.F., Marshall H.L., Antia B., et al., 1994, AJ 107, 751
Mekkadan M.V., Raveendran A.V., Mohin S., 1980, IBVS 1791
Mitrou C.K., Doyle J.G., Mathioudakis M., Antonopoulou E., 1996, A&AS 115, 61
Mitrou C.K., Mathioudakis M., Doyle J.G., Antonopoulou E., 1997, A&A 317, 776
Montes D., Fernandez-Figueroa M.J., de Castro E., Sanz-Forcada J., 1997, A&AS 125, 263
Nadal R., Pedoussaut A., Ginestet N., Carquillat J.-M., 1974, A&A 37, 191
Osawa K., 1959, ApJ 130, 159
Ossendrijver A.J.H., 1997, A&A 323, 151
Osten R.A., Brown A., 1999, ApJ 515, 746
Pavlovski K., Harmanec P., Bozic H., et al., 1997, A&AS 125, 75
Perry C.L., Olsen E.H., Crawford D.L., 1987, PASP 99, 1184
Perryman M.A.C., Lindegren L., Kovalevsky J., et al., 1997, A&A 323, L49
Pounds K.A., Allan D.J., Barber C., et al., 1993, MNRAS 260, 77
Pulkkinen P., Tuominen I., 1998, A&A 332, 748
Simon T., Fekel F.C., 1987, ApJ 316, 434
Slettebak A., 1954, ApJ 119, 146
Slettebak A., 1982, ApJS 50, 55
Strassmeier K.G., 1996, In: Strassmeier K.G., Linsky J.L. (eds.) Stellar Surface Structure. IAU Symp. 176, Kluwer Academic Publishers, Dordrecht, p. 289
Strassmeier K.G., Hall D.S., Boyd L.J., Genet R.M., 1989, ApJS 69, 141
Strassmeier K.G., Fekel F.C., Bopp B.W., Dempsey R.C., Henry G.W., 1990, A&AS 72, 191
Swanepoel J.W.H., De Beer C.F., 1990, ApJ 350, 754
Willson R.C., Hudson H.S., 1991, Nat 351, 42